1
2
3
4
5
6
7
8
9
10
11
12
13
14
15
16
17
18
19
20
21
22
23
24
25
26
27
28
29
30
31
32
33
34
35
36
37
38
39
40
41
42
43
44
45
46
47
48
49
50
51
52
53
54
55
56
57
58
59
60

Table 1. Expression of surface epitopes in MPC-selected cells

Surface epitoptes	MPC 0%	MPC 1%	MPC 2%	MPC 5%	MPC 10%
CD29 (Integrin β1)	++	++	+++	++	++
CD44 (Hyaluronan receptor)	++	++	++	++	++
CD105 (Endoglin)	+	+	+	+	+
CD166 (ALCAM)	+	+	+	+	+
CD34	-	-	-	-	-
CD45 (LCA)	-	-	-	-	-

214x279mm (300 x 300 DPI)

Superlubricious surface mimicking articular cartilage by grafting poly(2-methacryloyloxyethyl phosphorylcholine) on orthopaedic metal bearings

Masayuki Kyomoto,[1,2,3] Toru Moro,[3,4] Yasuhiko Iwasaki,[5] Fumiaki Miyaji,[1] Hiroshi Kawaguchi,[4] Yoshio Takatori,[3,4] Kozo Nakamura,[3] Kazuhiko Ishihara[2,6]

[1]Research Department, Japan Medical Materials Corporation, Osaka, Japan
[2]Department of Materials Engineering, School of Engineering, The University of Tokyo, Tokyo, Japan
[3]Division of Science for Joint Reconstruction, School of Medicine, The University of Tokyo, Tokyo, Japan
[4]Department of Orthopaedic Surgery, Faculty of Medicine, The University of Tokyo, Tokyo, Japan
[5]Department of Chemistry and Materials Engineering, Faculty of Chemistry, Materials and Bioengineering,
Kansai University, Osaka, Japan
[6]Center for NanoBio Integration, The University of Tokyo, Tokyo, Japan

Abstract: Aseptic loosening of the artificial hip joint with osteolysis due to the wear particles from polyethylene cup has remained as a serious issue. To reduce this wear and develop a novel artificial hip joint system, we produced a superlubricious metal-bearing material: for this, we grafted a 2-methacryloyloxyethyl phosphorylcholine (MPC) polymer onto the surface of a cobalt–chromium–molybdenum (Co-Cr-Mo) alloy. For ensuring long-term benefit retention of poly(MPC) on the Co-Cr-Mo alloy for application as a novel artificial hip joint system, several issues must be considered: strong bonding between poly(MPC) and Co-Cr-Mo surface, high mobility of free end groups of the poly(MPC) layer, and high density of the introduced poly(MPC). Considering these issues, we introduced a 3-methacryloxypropyl trimethoxysilane (MPSi) intermediate layer and a photoinduced graft polymerization technique to create a strong covalent bond between the Co-Cr-Mo substrate and the poly(MPC) chain via the MPSi layer. The thickness and density of the poly(MPC) layer on the surface increased with the MPC concentration and photoirradiation time. The grafted poly(MPC) layer successfully provided super-lubricity to the Co-Cr-Mo surface. The poly(MPC)-grafted crosslinked polyethylene/poly(MPC)-grafted Co-Cr-Mo or cartilage/poly(MPC)-grafted Co-Cr-Mo bearing interface mimicking natural joints showed an extremely low friction coefficient of 0.01, which is as low as that of natural cartilage interface. A superlubricious metal-bearing surface would enable the development of a novel biocompatible artificial hip joint system-artificial femoral head for partial hemiarthroplasty and metal-on-polymer/metal type for total hip arthroplasty. © 2008 Wiley Periodicals, Inc. J Biomed Mater Res 00A: 000–000, 2008

Key words: joint replacement; metal surface treatment; photopolymerization; phosphorylcholine; hydrophilicity

INTRODUCTION

Every year, the number and prevalence of primary and revision hip and knee joint replacements increases substantially worldwide.[1] As a result, the quality of artificial joints is becoming increasingly important. Most patients who receive an artificial joint experience dramatic pain relief and rapid improvement in both their daily activities and qual-

Correspondence to: M. Kyomoto, Uemura Nissei Bldg. 9F, 3-3-31 Miyahara, Yodogawa-ku, Osaka 532-0003, Japan; e-mail: kyomotom@jmmc.jp

ity of life. The most widely used bearing couple in artificial hip joint systems is a combination of an ultrahigh molecular weight polyethylene (UHMWPE) acetabular component and a metal femoral component. Cobalt–chromium–molybdenum (Co-Cr-Mo) alloy is one of the most widely used metal bearing materials in artificial joint systems. The Co-Cr-Mo alloy has good mechanical properties, castability, corrosion resistance, and wear resistance, whereas stainless steel and titanium alloys have a disadvantage with regard to corrosion resistance and wear resistance, respectively.

In total hip arthroplasty (THA), osteolysis caused by the wear particles from UHMWPE has been recognized as a serious issue.[2–4] Efforts to decrease

these particles have focused on bearing material improvement and the use of combinations other than metal-on-UHMWPE.[5-7] Recently, a metal-on-metal type artificial hip joint system consisting of Co-Cr-Mo acetabular and femoral components has been studied.[8] The advantages of the Co-Cr-Mo/Co-Cr-Mo bearings are that they do not generate UHMWPE wear debris and they exhibit decreased wear when compared with Co-Cr-Mo/UHMWPE bearings.[9,10] However, even in Co-Cr-Mo/Co-Cr-Mo bearings, aseptic loosening induced by wear particles and metallosis remains as serious issue in revision surgeries.[11,12] In addition to metallosis, electrochemical corrosion and carcinogenesis occurring due to the dissemination of wear particles to the other parts of the body have been reported.[13]

On the other hand, improvements in the bearing materials and surface modifications of the Co-Cr-Mo alloy have been attempted, in order to reduce such wear particles.[14,15] Surface coating may reduce the wear without compromising the bulk mechanical properties of the implant materials. Various "hardening treatments" of metal bearing surfaces, such as diamond-like carbon coating, titanium nitride coating, and ion implantation have also been attempted.[16,17] Although these surface modifications may improve THA survivorship, the limited THA longevity imposes restrictions for its application to younger patients. Consequently, the possibility of replacing the femoral head alone, whether solid or articular surface replacement, remains an attractive feature of such implants during revision surgeries of THA. However, the Co-Cr-Mo alloy or the hardening-treated Co-Cr-Mo alloy may induce damage to cartilaginous tissue.

In contrast, the previous study reported that highly lubricious hydrogel polymer used as an artificial cartilage did not damage cartilaginous tissue.[18] We have recently developed a highly lubricious artificial hip joint system by a "mild treatment" with soft materials. In this treatment, poly(2-methacryloyloxyethyl phosphorylcholine) (MPC) was grafted onto the surface of CLPE (CLPE-g-MPC).[19-21] MPC is a methacrylate with a phospholipid polar group in a side chain, and it has both good solubility in polar solvents including water and polymerization ability by conventional radical polymerization.[22] Many MPC polymers have been widely investigated as biomaterials.[23-27] As a result, various medical devices have already been developed using MPC polymers, and they are being used clinically. The efficacy of MPC polymers as biomaterials has been well verified.[28-30]

In general, there are two methods for modifying the polymer surface. The first method involves surface absorption or reaction with small molecules,[31,32] and the second is grafting polymeric molecules onto the substrate through covalent bonding.[33] Most frequently, grafting polymerization is performed using either of the following methods: (1) surface-initiated graft polymerization, termed as the "grafting from" method, in which monomers are polymerized from initiators or comonomers and (2) adsorption of the polymer to the substrate, termed as the "grafting to" method (i.e., dipping, crosslinking, and ready-made polymers with reactive end groups reacting with the functional groups of the substrate).[34,35] In our previous study, the Co-Cr-Mo-g-MPC prepared by the adsorption of the polymer to the Co-Cr-Mo substrate, termed as the "grafting to" method, was not uniform, and the CLPE-g-MPC/Co-Cr-Mo-g-MPC bearing couples showed high friction.[36] These results were probably ascribed to a low density of the poly(MPC) on Co-Cr-Mo prepared by the "grafting to" method. To solve the issue in this study, we developed a superlubricious surface with nanometer-scale poly(MPC) modification and was accomplished by using a photo-induced radical polymerization technique that was similar to the one used in the "grafting from" method. The "grafting from" method has an advantage over the "grafting to" method in that it synthesizes a high-density polymer brush.

To ensure *in vivo* long-term retention of this poly(MPC) graft on the Co-Cr-Mo alloy, it is necessary to create strong covalent bonding between the Co-Cr-Mo alloy substrate and the poly(MPC) graft chain. Organosilanes have already been known as surface coupling agents to enhance bonding between a metal or a metal oxide surface and an organic resin such as dental resin, and they can strongly bind metals to resins in dental implants.[37] Organic silanes or silane coupling agents comprise at least a hydrolyzable alkoxysilyl or chlorosilyl group and an organo-functional group.[38] The agents are effective to introduce organofunctional groups into the siloxane network polymer. The organofunctional group in the silane could be useful to improve bonding with the organic overlayer. 3-Methacryloxypropyl trimethoxysilane (MPSi) is a simple surface coupling agent consisting of three methoxysilane groups, a propyl chain, and a functional methacrylate, and the structure of its main chain is equivalent to that of MPC.

In this study, based on the hypothesis that the "grafting from" method has advantages over the "grafting to" method in that it can synthesize a uniformly and controllable polymer layer, a superlubricious metal bearing material in which the poly(MPC) with biocompatibility and hydrophilicity was grafted onto the surface of the Co-Cr-Mo alloy (Co-Cr-Mo-g-MPC) has been introduced for developing a novel artificial hip joint system, that is, artificial femoral head and metal-on-metal (Co-Cr-Mo/Co-Cr-Mo) type for THA. The surface structure and preliminary tribological properties of Co-Cr-Mo-g-MPC were also investigated.
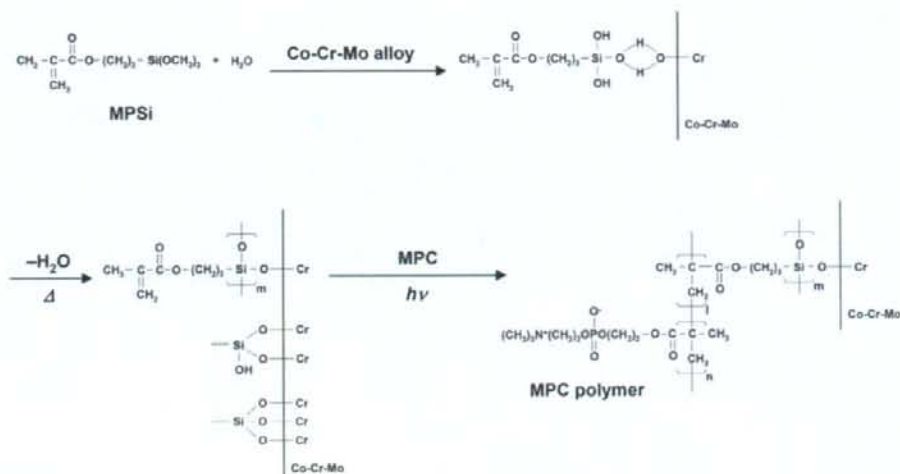
Figure 1.   Chemical reaction on Co-Cr-Mo during polymerization of MPC.

MATERIALS AND METHODS

Chemicals

MPC was synthesized industrially by using the method developed by Ishihara et al.,[22] and it was supplied by AI Bio-Chips Co., Ltd. (Tokyo, Japan). MPSi was purchased from Shin-Etsu Chemical Co., Ltd. (Tokyo, Japan). Succinic acid and ethanol were purchased from Kanto Chemical Co., Inc. (Tokyo, Japan). 2-Hydroxy-l-[4-(hydroxyethoxy)phenyl]-2-methyl-lpropanone (DAROCUR® 2959; D2959) was purchased from Ciba Specialty Chemicals Holding Inc. (Basel, Switzerland). D2959 is a highly efficient radical photoinitiator for ultraviolet (UV) curing of the systems containing unsaturated monomers and prepolymers, and it is particularly well known as a cytocompatible UV photoinitiator with UV intensities of <6 mW/cm² that can perform polymerization for up to 10 min with a UV light of 365 nm.[39]

Co-Cr-Mo alloy substrate and pretreatments

The Co-Cr-Mo alloy was supplied by Yoneda Advanced Casting Co., Ltd (Takaoka, Japan). This alloy was manufactured according to the ASTM F75 standard specification for Co-28Cr-6Mo alloy.[40] The Co-Cr-Mo samples were polished so that the average surface roughness ranged between 0.01 and 0.02 μm.

The polished Co-Cr-Mo samples were washed with acetone and then immersed in 35 vol % nitric acid at room temperature for 35 min according to the ASTM F86-04 standard.[36,41] This treatment results in passivation by surface oxidation, and it could lead to the dissolution of certain foreign materials that may remain from the previous procedure. Moreover, a previous study reported that the surface of as-polished Co-Cr-Mo alloy might lack the Cr content that the bulk possesses, and that surface etching

by nitric acid treatment would have produced a Cr-rich surface layer.[36] We therefore treated the surface with nitric acid with the aim of increasing the Cr concentration by "resurfacing."

After the nitric acid treatment, the Co-Cr-Mo samples were irradiated with O₂ plasma at a 500-W high-frequency output and 150-mL/min O₂ gas flow for 5 min by using an O₂ plasma etcher (PR500, Yamato Scientific Co., Ltd., Tokyo, Japan). The O₂ plasma treatment increased the thickness of the surface oxide layer.[42]

MPSi silanization and MPC graft polymerization

The synthesis of Co-Cr-Mo-g-MPC is schematically illustrated in Figure 1. The pretreated Co-Cr-Mo samples were immersed in an ethanol solution containing 5 mass % MPSi, 1 mass % succinic acid, and 0.1 mass % D2959 at room temperature for 12 h for silanization of the trimethoxysilane group. In this study, D2959 was used as a photoinitiator for surface-initiated polymerization so as to be included in the MPSi layer. Generally, for surface-initiated polymerization, such an initiator covalently bonded to the substrate to yield a "grafting from" polymerization is usually used. They were then annealed at 70°C for 3 h in air for dehydration. The MPC was dissolved in degassed pure water to attain concentrations ranging from 0.25 to 1.00 mol/L. Subsequently, the MPSi (containing D2959)-coated Co-Cr-Mo samples were immersed in aqueous MPC solutions. Photoinduced graft polymerization on the Co-Cr-Mo surface was performed using ultraviolet irradiation (UVL-400HA ultra-high pressure mercury lamp; Riko-Kagaku Sangyo Co., Ltd., Funabashi, Japan) with an intensity of 5 mW/cm² at 60°C for 23–180 min; a filter (Model D-35; Toshiba Corp., Tokyo, Japan) was used restrict the passage of ultraviolet light to wavelengths of 350 ± 50 nm. After the polymerization, the Co-Cr-Mo-g-MPC samples were removed from the solution, washed with pure water and

ethanol, and dried at room temperature. For purification, washing with pure water and ethanol enables the removal of the free poly(MPC) and/or poly(MPC-co-MPSi) adsorbed on the Co-Cr-Mo surface.[43]

MPC graft polymerization on crosslinked polyethylene

Compression-molded UHMWPE (GUR1020 resin, Poly Hi Solidur Inc., IN) bar stock was gamma-ray irradiated at 50 kGy in N_2 gas and annealed at 120°C in N_2 gas for crosslinking. After cooling, the crosslinked polyethylene (CLPE) specimens were machined from this bar stock.

MPC grafting onto the CLPE surface was performed as described in previous studies.[43–45] The CLPE specimens were immersed in an acetone solution containing 10 mg/mL benzophenone for 30 s and then dried in the dark at room temperature to remove the acetone. MPC was dissolved in degassed pure water to a concentration of 0.5 mol/L. The benzophenone-coated CLPE samples were immersed in the aqueous MPC solution. Photoinduced graft polymerization on the CLPE surface was carried out using UV irradiation with an intensity of 5 mW/cm² at 60°C for 90 min. After the polymerization, the CLPE-g-MPC samples were removed from the solution, washed with pure water and ethanol, and dried.

Articular cartilage from porcine ankle joint

Using a surgical hand corer or surgical saw, articular cartilage specimens were harvested from the flat part of the ankle joint of the fresh frozen porcine tibia (ages 6–9 months) for friction test. Pin-type articular cartilage specimens were shaped as cylinders with a height of 5 mm and diameter of 9 mm, and they had ~1 mm of cartilage layer and subcondral bone used for mounting. Throughout the procedure, the articular cartilage surface was hydrated regularly with Dulbecco's phosphate-buffered saline (PBS, pH 7.4, ion strength = 0.15 M; Immuno-Biological Laboratories Co., Ltd., Takasaki, Japan). All the articular cartilage specimens were then stored in Dulbecco's PBS and frozen at −80°C.[46]

Surface analysis by Fourier transform infrared spectroscopy, X-ray photoelectron spectroscopy, and water-contact angle measurement

The functional group vibrations of the Co-Cr-Mo alloy surfaces before and after the MPC grafting were examined by Fourier-transform infrared (FTIR) spectroscopy with attenuated total reflection (ATR) equipment. The FTIR/ATR spectra were obtained using an FTIR analyzer (FT/IR615, JASCO Co. Ltd., Tokyo, Japan) for 32 scans (1.2 s/scan) over the range of 800–2000 cm⁻¹ at a resolution of 4.0 cm⁻¹.

The surface elemental conditions of the Co-Cr-Mo alloy before and after the MPC grafting were analyzed by X-ray photoelectron spectroscopy (XPS). The XPS spectra were obtained using an XPS spectrophotometer (AXIS-HSi165, Kratos Analytical Ltd., Manchester, UK) equipped with a 15-kV MgKα radiation source at the anode. The take-off angle of the photoelectrons was maintained at 90°. Five

scans (~260 to 425 s/scan depending on the atomic signal strength) were taken for each sample.

The static-water contact angles on the Co-Cr-Mo surfaces that were subjected to different types of pretreatments before and after the MPC grafting were measured by the sessile drop method using an optical bench-type contact angle goniometer (Model DM300, Kyowa Interface Science Co., Ltd., Saitama, Japan). Drops of purified water (1 μL) were deposited on the Co-Cr-Mo-g-MPC surface, and the contact angles were directly measured with a microscope after 60 s of dropping, according to the ISO 15989 standard.[47] Measurements were repeated six times for each sample, and the average values were considered as the contact angles.

Cross-sectional observation by transmission electron microscopy

A crosssection of the poly(MPC) layer on the Co-Cr-Mo surface was observed using a transmission electron microscope (TEM) and by energy dispersive X-ray (EDX) spectroscopy. The specimens were precoated with an aluminum film using a focused ion beam (FIB) system to prevent charging. After precoating, a thin film of the samples was prepared by the FIB technique using an FB-2000A (Hitachi High-Technologies Co., Tokyo, Japan) FIB system. The samples were thinned to electron transparency by a low gallium ion beam current. The thin film thus prepared was positioned onto a copper TEM mesh grid. TEM observations were then recorded using an HF-2000 electron microscope (Hitachi High-Technologies Co.) at an acceleration voltage of 200 kV. EDX spectra were analyzed on a crosssection of the untreated Co-Cr-Mo sample and the Co-Cr-Mo-g-MPC sample obtained with 0.50 mol/L MPC concentrations and a 90-min photoirradiation time using a Sigma EDX attachment (Kevex Instruments, Inc., Valencia, CA) at an acceleration voltage of 200 kV. The probe size of the electron beam was maintained at 1 nm.

Friction test

The coefficients of dynamic friction between the pins fabricated from various materials (Co-Cr-Mo, CLPE, CLPE-g-MPC, and articular cartilage) and the untreated Co-Cr-Mo or Co-Cr-Mo-g-MPC (obtained with 0.50 mol/L MPC concentrations and a 90-min photoirradiation time) plates were measured using a pin-on-plate machine (Tribostation 32; Shinto Scientific Co., Ltd., Tokyo, Japan) as the preliminary test for tribological properties. Each pin was a cylinder measuring 5 mm in height and 9 mm in diameter and used to prepare five sample pieces. The friction tests were performed at room temperature with a load of 0.98 N, sliding distance of 25 mm, and frequency of 1 Hz for a maximum of 100 cycles.[48] Pure water was used as a lubricant. The mean coefficients of dynamic friction were determined by averaging five data points from the 100 (96–100) cycle measurements. Standard analysis of variance (ANOVA) was applied to the data of the (at 100 cycles) existed among the eight groups (Co-Cr-Mo, CLPE, CLPE-g-MPC, Cartilage pins against untreated Co-Cr-Mo and Co-Cr-Mo-
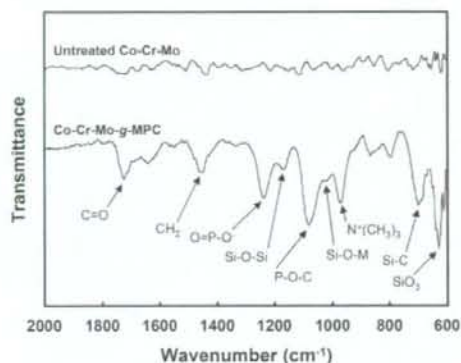
Figure 2. FTIR/ATR spectra of untreated Co-Cr-Mo and Co-Cr-Mo-g-MPC surfaces with a 0.50-mol/L MPC concentration and a 90-min photoirradiation time.

g-MPC plates, respectively), in this study. Two combinations (e.g., Co-Cr-Mo pin against untreated Co-Cr-Mo and Co-Cr-Mo-g-MPC plates, Co-Cr-Mo and CLPE pins against Co-Cr-Mo-g-MPC plate) were especially made with the Student's t test ($p < 0.05$).

RESULTS

Figure 2 shows the FTIR/ATR spectra of the Co-Cr-Mo sample and that of photoirradiated grafting of MPC under 0.50-mol/L MPC concentration and 90-min photoirradiation time. Absorption peaks were not observed for the Co-Cr-Mo sample before the MPC graft polymerization in the wavenumber

range of 800–2000 cm^{-1}. In contrast, absorption peaks were newly observed only for the Co-Cr-Mo-g-MPC samples. The peaks at 1720, 1550, and 1460 cm^{-1} are attributed to C=O and —CH_2— in the MPSi and poly(MPC) graft chains. The peaks at 1180, 1040, 700, and 630 cm^{-1} are attributed to the trimethoxysilane group in the MPSi unit.[49] The peaks at 1240, 1080, and 970 cm^{-1} are attributed to the -$N^+(CH_3)_3$ and phosphate groups in the MPC unit.[44]

In the XPS spectra of the binding energy region of the nitrogen (N_{1s}), phosphorous (P_{2p}), and silicon (Si_{2p}) electrons, peaks appeared in the case of Co-Cr-Mo-g-MPC; however, they were not observed in the case of Co-Cr-Mo (Fig. 3). The peak at 104 eV was attributed to the Si_2O_3 or SiO_2 in the trimethoxysilane group in the MPSi unit. The peaks at 403 and 134 eV were attributed to the —$N^+(CH_3)_3$ and phosphate groups, respectively. These peaks reflect the phosphorylcholine present in the MPC units. Figure 4 shows the Si, N, and P concentrations of the Co-Cr-Mo-g-MPC surface as a function of the photoirradiation time during polymerization for various MPC concentrations in feeds. Both the N and P concentrations in the Co-Cr-Mo-g-MPC surface increased with the photoirradiation time. In the case of higher MPC concentrations, when the photoirradiation time was greater than 90 min, the N and P concentrations became almost constant above 5.0 atom%. These values were almost equivalent to the theoretical elemental composition (N = 5.3 atom%, P = 5.3 atom%) of poly(MPC). As a trade off, the Si concentration at the Co-Cr-Mo-g-MPC surface decreased with an increase in the photoirradiation time.
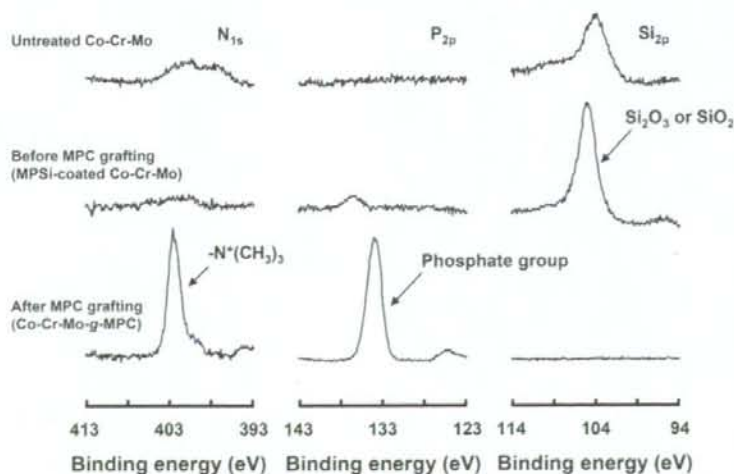

Figure 3. XPS spectra (N_{1s}, P_{2p} and Si_{2p}) of Co-Cr-Mo samples before and after the MPC grafting with a 0.50-mol/L MPC concentration and a 90-min photoirradiation time.
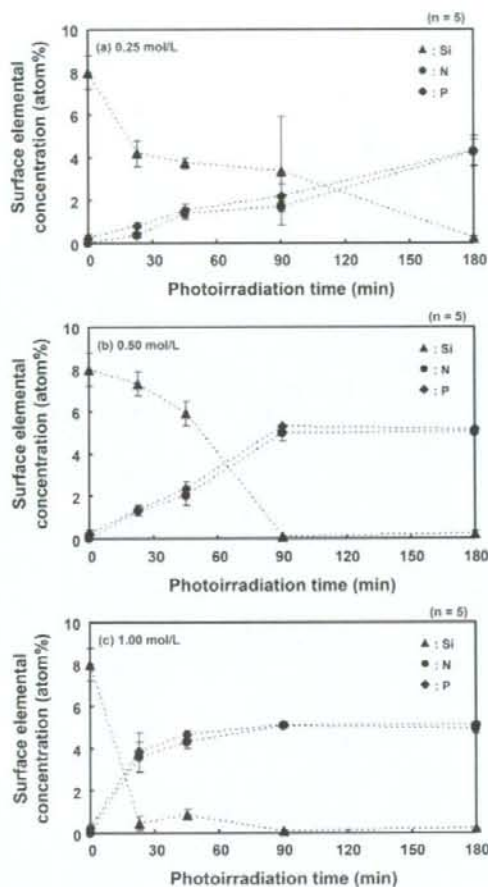
Figure 4. Surface elemental concentrations in the Co-Cr-Mo-*g*-MPC surface as a function of the photoirradiation time for various MPC concentrations in feeds. Bar: standard deviations.

F5   Figure 5 shows the static-water contact angle on the Co-Cr-Mo-*g*-MPC surface as a function of the photoirradiation time during polymerization with various MPC concentrations in feeds. The static-water contact angle on the untreated Co-Cr-Mo surface before the MPC grafting was ~80°. The static-water contact angle on the Co-Cr-Mo-*g*-MPC surface decreased markedly with an increase in the photoirradiation time and the MPC concentration. When the photoirradiation time and MPC concentration were greater than 90 min and 0.50 mol/L, respectively, the static-water contact angle became constant at a low value of 20°.

F6   Figure 6 shows the cross-sectional TEM images of Co-Cr-Mo-*g*-MPC obtained with various MPC con-

centrations and a 90-min photoirradiation time. In the Co-Cr-Mo-*g*-MPC, a 10 to 360-nm thick poly (MPC) layer was clearly observed on the surface of the Co-Cr-Mo substrate. The thickness of the poly (MPC) layer increased with the MPC concentration during polymerization. At an MPC concentration of 1.00 mol/L, the thickness of the poly(MPC) layer was greatest, that is, 360 nm. These results indicate that the length of the poly(MPC) chain (thickness of the poly(MPC) layer) can be controlled by adjusting the MPC concentration during polymerization. This is explained by the fact that the length of the polymer chains produced in a radical polymerization reaction generally correlates with the MPC concentration.

Figure 7 shows the EDX spectra of the untreated   F7
Co-Cr-Mo and Co-Cr-Mo-*g*-MPC obtained with a 0.5-mol/L MPC concentration and a 90-min photoirradiation time. In spectra (P1) and (P3) of the substrate of the untreated Co-Cr-Mo and Co-Cr-Mo-*g*-MPC, strong peaks were observed at 0.8, 2.3, 5.4, 6.0, 6.9, and 7.7 keV. These peaks are attributed to the Co, Cr, and Mo atoms in the Co-Cr-Mo substrate. In spectrum (P2) of the surface of the untreated Co-Cr-Mo, a peak was observed at 0.5 keV. This peak is attributed to the O atom in the metal oxide layer of the Co-Cr-Mo. In spectrum (P4) of the intermediate layer of the Co-Cr-Mo-*g*-MPC, peaks were observed at 0.5 and 1.7 keV. These peaks are attributed to the O and Si atoms in the intermediate layer between the silane of the MPSi and the metal oxide of the Co-Cr-Mo. In spectra (P4) and (P5) of the intermediate layer and the poly(MPC) layer of the Co-Cr-Mo-*g*-MPC, a significant peak attributed to the P atom was observed at 2.0 keV. This peak is mainly attributed to the MPC units. Several spectra exhibited
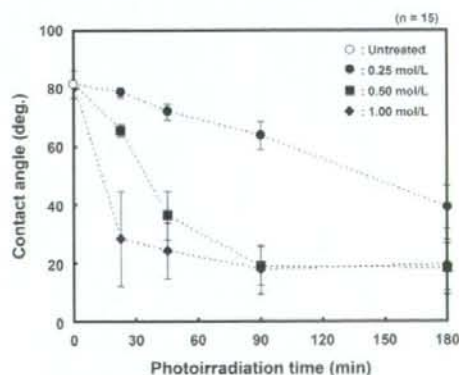

Figure 5. Static-water contact angle of the Co-Cr-Mo-*g*-MPC surface as a function of the photoirradiation time for various MPC concentrations in feeds. Bar: standard deviations.
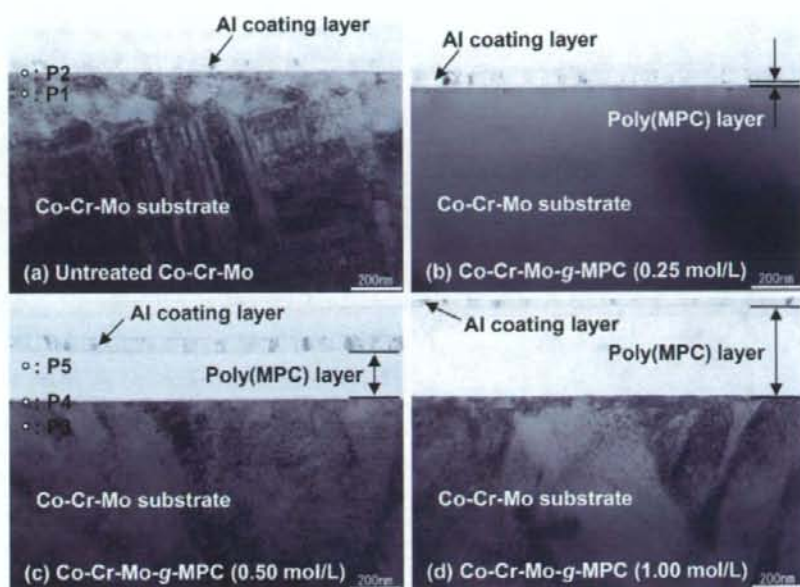
Figure 6. Cross-sectional TEM images of the Co-Cr-Mo-g-MPC surface with various MPC concentration in feeds and a 90-min photoirradiation time. Aluminun coating layers (~70 nm) for preparation of TEM observation specimen are shown above the poly(MPC) layer of the Co-Cr-Mo-g-MPC surface. In (a) and (c), small open-circles (P1-5) indicate EDX analysis points. Bar: 200 nm.

peaks at 1.5, 8.0, and 8.9 keV. In these cases, the peaks are attributed to the Al and Cu atoms of the Aluminum coating for the preparation of the TEM observation specimen and/or the copper TEM mesh grid.

Figure 8 shows the coefficients of dynamic friction of the sliding couples, namely, untreated Co-Cr-Mo, CLPE, CLPE-g-MPC, and articular cartilage pins sliding against the untreated Co-Cr-Mo and Co-Cr-Mo-g-MPC plates. The Co-Cr-Mo/Co-Cr-Mo and CLPE/Co-Cr-Mo couples showed a high friction coefficient of ~0.19 and 0.14 in the initial 10 cycles; especially, the value of the Co-Cr-Mo/Co-Cr-Mo couple increased and reached ~0.41 in the 100 cycles ($p <$ 0.005). After the friction test, some scratches parallel to the sliding direction were clearly observed in the Co-Cr-Mo/Co-Cr-Mo bearing area. The CLPE-g-MPC/Co-Cr-Mo couples showed a low friction coefficient of about 0.05 for both 10 and 100 cycles. This corresponds to ~70% reduction ($p <$ 0.001 in both cycles) when compared with the coefficients of untreated CLPE/Co-Cr-Mo couples. The coefficients of dynamic friction of all types of pins sliding against the Co-Cr-Mo-g-MPC couples decreased drastically when compared with those of untreated Co-Cr-Mo couples. The degree of reduction in the coefficient was ~90% (80–99%) for both 10 and 100

cycles ($p <$ 0.001 in all types of pins). In particular, in the CLPE-g-MPC/Co-Cr-Mo-g-MPC couple, the poly(MPC) layer sliding against the poly(MPC) layer showed the lowest friction coefficient of ~0.005, and this value was almost steady during the experiment. The friction coefficient of the cartilage/Co-Cr-Mo couple increased gradually and reached ~0.09 in the 100 cycles. The friction coefficient of the cartilage/Co-Cr-Mo-g-MPC couple was ~0.006 in the 100 cycles, and it remained almost steady. This was much lower than the friction coefficient of the cartilage/Co-Cr-Mo couple ($p <$ 0.001).

DISCUSSION

In this study, based on the hypothesis that the "grafting from" method has advantages over the "grafting to" method in that it synthesizes a uniformly and controllable polymer layer, a superlubricious Co-Cr-Mo alloy surface by poly(MPC) grafting was prepared for its application to artificial joints with the aim of reducing wear. Several important issues are involved in the long-term retention of the benefits of poly(MPC) used in artificial joints under variable and multidirectional loads: strong bonding
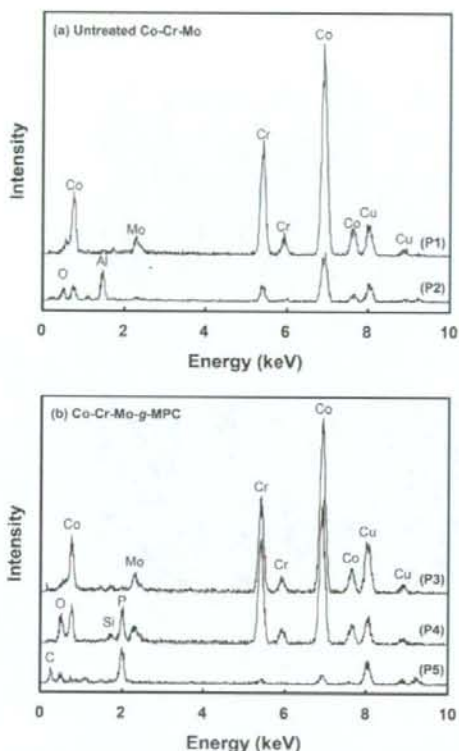
8   KYOMOTO ET AL.

Figure 7. EDX spectra of the Co-Cr-Mo-g-MPC surface with a 0.5-mol/L MPC concentration and a 90-min photo-irradiation time. The spectra were analyzed on the cross-section (P1–5) of the untreated Co-Cr-Mo and Co-Cr-Mo-g-MPC in Figure 6.

Mo substrate only, as shown in Figure 7. Therefore, it was thought that the poly(MPC) chain was grafted and that it extended from the methacrylate on the MPSi. The hydrophilic layer was formed with the poly(MPC) chain, which attained high mobility, and the poly(MPSi) chain existed as the immobilized end-group of the poly(MPC) graft chains.

In Figure 4, both the N and P concentrations in the Co-Cr-Mo-g-MPC surface attributed to poly (MPC) increased with the MPC concentration during polymerization. In addition, in the TEM images shown in Figure 6, the thickness of the poly(MPC) layer increased with the MPC concentration. When the poly(MPC) layer has a brush-like structure, the layer thickness may correlate with the molecular weight of the grafted poly(MPC). The high-density poly(MPC) graft chains in the Co-Cr-Mo-g-MPC are assumed to exhibit a brush-like structure.[24,50] It is generally well known that the reaction rate of radical polymerization is extremely high.[51] In this study, the length (molecular weight) of the poly(MPC) graft chains was successfully controlled by the MPC concentration used for polymerization as a feed solution. This indicates that the length of the poly(MPC) chain grafted on the Co-Cr-Mo surface increased with the MPC concentration in feed.[45]

The previous study by the authors reported that the density of the poly(MPC) chains on the surface of the CLPE prepared by photoinduced radical p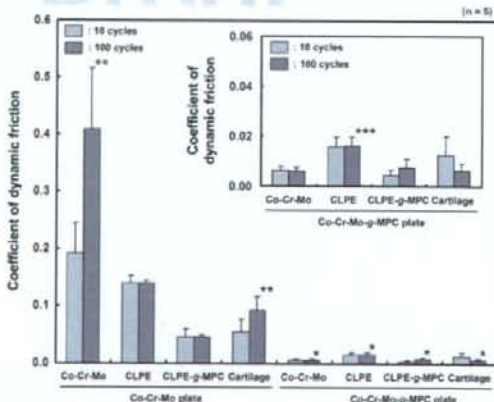olymerization gradually increased with the irradiation between the poly(MPC) and the Co-Cr-Mo surface, high mobility of the free end groups of the poly (MPC) layer, and a high density of the introduced poly(MPC). Taking these issues into consideration, the photoinduced radical graft polymerization technique and the MPSi intermediate layer were used to obtain covalent bonding between the Co-Cr-Mo substrate and the poly(MPC) chain via the MPSi layer.

Figure 4 shows the N and P concentrations of the Co-Cr-Mo-g-MPC surface obtained with a 0.5-mol/L MPC concentration and a 90-min photoirradiation time; the concentrations became almost constant at high values of 5.0 and 5.3 atom%, respectively. These values were almost equivalent to the theoretical elemental composition of poly(MPC). In addition, the static-water contact angle of the Co-Cr-Mo-g-MPC surface became constant at a low value of 20°, showing a highly hydrophilic nature. The peak attributed to Si atoms was observed in the intermediate layer between the poly(MPC) layer and Co-Cr-

Figure 8. Coefficients of dynamic friction for the various types of pins sliding against the untreated Co-Cr-Mo and Co-Cr-Mo-g-MPC plates. Bar: standard deviations. *t test, significant difference ($p < 0.001$) when compared with the untreated Co-Cr-Mo plate, **t test, significant difference ($p < 0.001$) when compared with the coefficients of dynamic friction at 10 cycles, and ***t test, significant difference ($p < 0.001$) when compared with the Co-Cr-Mo pin against Co-Cr-Mo-g-MPC plate.

time. The study also showed that the entire surface of the CLPE was coated using polymerization times longer than 45 min with almost the same thickness as that of the poly(MPC) layer for longer irradiation times (100–200 nm).[44] In this study, both the N and P concentrations in the Co-Cr-Mo-g-MPC surface attributed to poly(MPC) increased with the photoirradiation time. When the MPC concentration was greater than 0.5 mol/L, the N and P concentrations of the Co-Cr-Mo-g-MPC surface increased to ~5.3 atom%, which was almost equivalent to the theoretical elemental composition of poly(MPC). In addition, the Co-Cr-Mo-g-MPC surface obtained with a 0.5-mol/L MPC concentration and a 90-min photoirradiation time retained the uniform poly(MPC) layer with a thickness of 200 nm, as reported in the previous study. These observations indicate that irradiation time control is essential to obtain a high-density poly(MPC) layer.[44]

Several previous studies reported that a silane coating has a low water resistance due to hydrolysis of siloxane bond and to desorption of physisorbed silane. Zhang et al.[52] and others[53,54] reported that the limited stability of the Si—O—metal (M) bond against hydrolysis is the main reason for the limited stability in water, and the water stability could be improved by using several factors: (1) an induction of bridged silane coupling agents, when hydrolyzed, contain two or more –Si(OH)₃, (2) the hydrophobic alkyl moieties which limit the contact with water, and (3) a increase of thickness of surface oxide layer. Therefore, we used the MPSi intermediate layer with three methoxysilane groups and a functional methacrylate and the pretreatment (nitric acid treatment and O_2 plasma treatment) for Co-Cr-Mo surface were used.

MPSi binds to the Co-Cr-Mo substrate by a condensation reaction in two steps (Fig. 1). In the first step, the MPSi is hydrolyzed (activated), and in the second step, the hydrolyzed silane molecule binds to the surface by an Si-O—M bond, forming branched hydrophobic siloxane bonds, Si-O-Si.[38,49] The hydrolyzed silane molecule has three —OH groups that can react with the —OH groups of the surface metallic oxide layer to form siloxane bonds covalently. The peaks at 1180 and 1040 cm^{-1} in the FTIR/ATR spectrum of the Co-Cr-Mo-g-MPC surface were attributed to Si—O—Si and Si—O—M, respectively (Fig. 2), and these were observed after the MPC grafting. This suggests that the trimethoxysilane group of MPSi binds to the metallic oxides with a stable covalent binding even when the polymerization of MPC was carried out. This MPSi (and/or poly(MPC-co-MPSi)) layer(s) and the Co-Cr-Mo substrate might contribute to the stable polymer/metal interface.[55]

The coefficients of dynamic friction of various bearing couples obtained in previous studies are

TABLE I
Coefficients of Dynamic Friction of Various Bearing Couples in Previous Studies

Bearing Couple		Friction Coefficient	Reference
Pin	Disc or Plate		
Co-Cr-Mo	Co-Cr-Mo	0.19–0.27	36, 56
UHMWPE	Co-Cr-Mo	0.05–0.13	36, 57, 58
CLPE-g-MPC	MPC "grafted to" Co-Cr-Mo	0.07–0.13	36
Cartilage	Stainless steel	0.01–0.05	61
Cartilage	Cartilage	0.02	62

summarized in Table I. In Figure 8, the Co-Cr-Mo/ Co-Cr-Mo couple shows a friction coefficient of ~0.19, which is as high as that described in previous studies.[36,56] The CLPE/Co-Cr-Mo couple also shows a friction coefficient of ~0.14, as high as that described in previous studies.[36,57,58] In contrast, the Co-Cr-Mo-g-MPC surface with respect to each material shows an extremely low friction coefficient when compared with that of the untreated Co-Cr-Mo surface. As MPC is highly hydrophilic and poly(MPC) is water soluble, the water contact angle of the Co-Cr-Mo-g-MPC surface was lower than that of the untreated Co-Cr-Mo surface, as shown in Figure 5. Consequently, the grafted poly(MPC) layer successfully provided high lubricity in the form of "surface gel hydration lubrication" to the Co-Cr-Mo surface (Fig. 8).[59]

Various factors such as the type of bearing material, surface roughness, homogeneity of the surface, and chemical composition affect the lubricity of artificial joints.[60] In Figure 8, the friction coefficient of the CLPE/Co-Cr-Mo-g-MPC couple was greater than that of Co-Cr-Mo/Co-Cr-Mo-g-MPC couple ($p < 0.001$ in both 10 and 100 cycles). The significant difference for the friction coefficient of those bearing couples was probably attributed to a surface roughness of bearing pin: although the bearing surface of Co-Cr-Mo pins was polished so that the average surface roughness (R_a) was ~0.01 μm, the bearing surface of CLPE pins was only machine-finished so that the R_a was ~20 μm. These bearing surfaces were actually comparable with those of femoral ball and acetabular cup products, respectively. However, if the bearing surface of CLPE pins was polished or direct molded like that of Co-Cr-Mo pins, the friction coefficient of the CLPE/Co-Cr-Mo-g-MPC couple would be similar to that of Co-Cr-Mo/Co-Cr-Mo-g-MPC couple.

In the case of Co-Cr-Mo-g-MPC, the lubricity changes depending on the ambient *in vitro* and *in vivo* conditions. The previous study reported that the hydrogel cartilage surface is assumed to have a brush-like structure: a part of the proteoglycan ag-
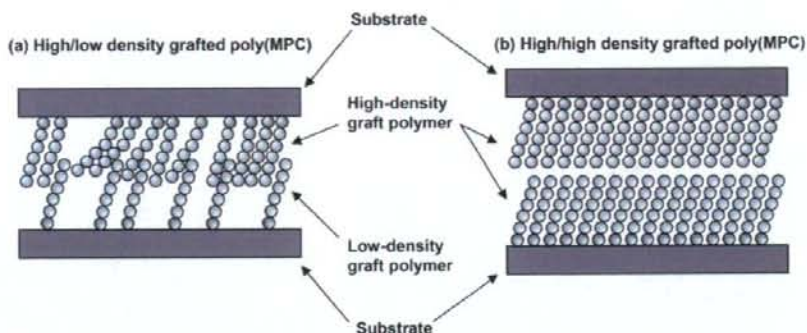
Figure 9. Hypothetical cartoons of high-density grafted poly(MPC)/low-density grafted poly(MPC) and high-density grafted poly(MPC)/high-density grafted poly(MPC) bearing interfaces.

gregate brush is bonded with the collagen network on the cartilage surface.[59] The bearing surface with poly(MPC) in artificial hip joints is assumed to have a brush-like structure similar to that of articular cartilage. CLPE-g-MPC/Co-Cr-Mo-g-MPC or cartilage/Co-Cr-Mo-g-MPC bearing couples can therefore be regarded to mimic the natural joint cartilage *in vivo*. The friction coefficient of cartilage/stainless steel (SUS) pin-on-plate ranges from 0.01 to 0.05,[61] and that of cartilage/cartilage pin-on-plate is 0.02,[62] as shown in Table I. In this study, it was found that CLPE-g-MPC/Co-Cr-Mo-g-MPC or cartilage/Co-Cr-Mo-g-MPC bearing couples mimic a natural joint, showed low friction (friction coefficient was ~0.01), as low as that of cartilage/SUS or cartilage/cartilage. Hence, it was considered that the Co-Cr-Mo-g-MPC surface is excellent for the femoral head articulating cartilage, because the cartilage/Co-Cr-Mo-g-MPC bearing couples showed a constant low friction coefficient of 0.006. We expect that the hemiarthroplasty with the Co-Cr-Mo-g-MPC femoral head bearing will be promising to preserve acetabular cartilage and extend the duration before THA in young patients.

On the other hand, in the previous study, the CLPE-g-MPC/Co-Cr-Mo-g-MPC prepared by the adsorption of the polymer to the substrate, termed as the "grafting to" method bearing couples showed high friction (friction coefficient was 0.12).[36] The poly(MPC) on Co-Cr-Mo used in this study might have a high density because the polymerization method used was surface-initiated graft polymerization, termed as the "grafting from" method, in which the monomers are polymerized from initiators or comonomers, whereas the poly(MPC) on Co-Cr-Mo prepared by the "grafting to" method might have a low density.[34,35] Figure 9 shows the hypothetical cartoons of high-density grafted poly(MPC)/low-density grafted poly(MPC) and high-density grafted poly(MPC)/high-density grafted poly(MPC) bearing

interfaces. The high-density grafted poly(MPC)/high-density grafted poly(MPC) bearing interface shows a remarkably lower friction than the high-density grafted poly(MPC)/low-density grafted poly(MPC) bearing interface.[63] Fukuda and coworkers reported that the friction of the bearing couple was higher in low-density polymer brushes than in high-density ones.[64] Therefore, it is assumed that a bearing couple with low-density poly(MPC) brushes may cause high friction by stick-slip motion with interpenetration, as shown in Figure 9(a).[63,65] In contrast, high-density poly(MPC) fabricated by the "grafting from" method may attain low friction, such as that in the case of "superlubricity," owing to resistance to interpenetration by volume effects resulting from chain mobility. The reduction in friction may contribute to the improvement in antiwear properties.[19–21] Although a hip joint simulator test is necessary to examine tribological advantages in human body environments, a superlubricious metal-bearing material would enable the development of a novel biocompatible artificial hip joint system-artificial femoral head for partial hemiarthroplasty and metal-on-polymer/metal type for THA.

CONCLUSION

We prepared a superlubricious metal-bearing material for application as a novel artificial hip joint system: poly(MPC) was grafted onto the surface of a Co-Cr-Mo alloy by employing a MPSi intermediate layer and by using the photoinduced radical graft polymerization technique. The thickness and density of the grafted poly(MPC) layer increased with the MPC concentration and photoirradiation time, respectively. In conclusion, the grafted poly(MPC) layer successfully provided superlubricity to the

Co-Cr-Mo surface, and the CLPE-*g*-MPC/Co-Cr-Mo-*g*-MPC or cartilage/Co-Cr-Mo-*g*-MPC bearing interface, which mimicked a natural joint, showed an extremely low friction coefficient of 0.01, a value that is as low as that of a natural cartilage interface.

References

1. Kurtz S, Mowat F, Ong K, Chan N, Lau E, Halpern M. Prevalence of primary and revision total hip and knee arthroplasty in the United States from 1990 through 2002. J Bone Joint Surg Am 2005;87:1487–1497.
2. Harris WH. The problem is osteolysis. Clin Orthop 1995;311: 46–53.
3. Kobayashi A, Freeman MA, Bonfield W, Kadoya Y, Yamac T, Al-Saffar N, Scott G, Revell PA. Number of polyethylene particles and osteolysis in total joint replacements. A quantitative study using a tissue-digestion method. J Bone Joint Surg Br 1997;79:844–848.
4. Sochart DH. Relationship of acetabular wear to osteolysis and loosening in total hip arthroplasty. Clin Orthop 1999; 363:135–150.
5. McKellop H, Shen FW, Lu B, Campbell P, Salovey R. Development of an extremely wear-resistant ultra high molecular weight polyethylene for total hip replacements. J Orthop Res 1999;17:157–167.
6. Muratoglu OK, Bragdon CR, O'Connor DO, Jasty M, Harris WH. A novel method of crosslinking ultra-high-molecular-weight polyethylene to improve wear, reduce oxidation, and retain mechanical properties: Recipient of the 1999 HAP Paul Award. J Arthroplasty 2001;16:149–160.
7. Urban JA, Garvin KL, Boese CK, Bryson L, Pedersen DR, Callaghan JJ, Miller RK. Ceramic-on-polyethylene bearing surfaces in total hip arthroplasty. Seventeen to twenty-one-year results. J Bone Joint Surg Am 2001;83:1688–1694.
8. McMinn DJ, Daniel J, Pynsent PB, Pradhan C. Mini-incision resurfacing arthroplasty of hip through the posterior approach. Clin Orthop Relat Res 2005;441:91–98.
9. Clarke IC, Good V, Williams P, Schroeder D, Anissian L, Stark A, Oonishi H, Schuldies J, Gustafson G. Ultra-low wear rates for rigid-on-rigid bearings in total hip replacements. Proc Inst Mech Eng [H] 2000;214:331–347.
10. Fisher J, Hu XQ, Stewart TD, Williams S, Tipper JL, Ingham E, Stone MH, Davies C, Hatto P, Bolton J, Riley M, Hardaker C, Isaac GH, Berry G. Wear of surface engineered metal-on-metal hip prostheses. J Mater Sci Mater Med 2004;15:225–235.
11. Keel JB, Kuster MS. Massive wear of an incompatible metal-on-metal articulation in total hip arthroplasty. J Arthroplasty 2004;19:638–642.
12. Korovessis P, Petsinis G, Repanti M, Repantis T. Metallosis after contemporary metal-on-metal total hip arthroplasty. Five to nine-year follow-up. J Bone Joint Surg Am 2006;88: 1183–1191.
13. Savarino L, Granchi D, Ciapetti G, Cenni E, Nardi Pantoli A, Rotini R, et al. Ion release in patients with metal-on-metal hip bearings in total joint replacement: A comparison with metal-on-polyethylene bearings. J Biomed Mater Res 2002;63: 467–474.
14. Dowson D, Hardaker C, Flett M, Isaac GH. A hip joint simulator study of the performance of metal-on-metal joints. I. The role of materials. J Arthroplasty 2004;19:118–123.
15. Bowsher JG, Nevelos J, Williams PA, Shelton JC. 'Severe' wear challenge to 'as-cast' and 'double heat-treated' large-diameter metal-on-metal hip bearings. Proc Inst Mech Eng [H] 2006;220:135–143.
16. Brizuela M, Garcia-Luis A, Viviente JL, Braceras I, Oñate JI. Tribological study of lubricious DLC biocompatible coatings. J Mater Sci Mater Med 2002;13:1129–1133.
17. Gutmanas EY, Gotman I. PIRAC Ti nitride coated Ti-6Al-4V head against UHMWPE acetabular cup-hip wear simulator study. J Mater Sci Mater Med 2004;15:327–330.
18. Oka M, Ushio K, Kumar P, Ikeuchi K, Hyon SH, Nakamura T, Fujita H. Development of artificial articular cartilage. Proc Inst Mech Eng [H] 2000;214:59–68.
19. Moro T, Takatori Y, Ishihara K, Konno T, Takigawa Y, Matsushita T, Chung UI, Nakamura K, Kawaguchi H. Surface grafting of artificial joints with a biocompatible polymer for preventing periprosthetic osteolysis. Nat Mater 2004;3:829–837.
20. Moro T, Takatori Y, Ishihara K, Nakamura K, Kawaguchi H. 2006 Frank Stinchfield Award: Grafting of biocompatible polymer for longevity of artificial hip joints. Clin Orthop Relat Res 2006;453:58–63.
21. Kyomoto M, Moro T, Konno T, Takadama H, Kawaguchi H, Takatori Y, Nakamura K, Yamawaki N, Ishihara K. Effects of photo-induced graft polymerization of 2-methacryloyloxyethyl phosphorylcholine on physical properties of cross-linked polyethylene in artificial hip joints. J Mater Sci Mater Med 2007;18:1809–1815.
22. Ishihara K, Ueda T, Nakabayashi N. Preparation of phospholipid polymers and their properties as polymer hydrogel membranes. Polym J 1990;22:355–360.
23. Ishihara K, Ziats NP, Tierney BP, Nakabayashi N, Anderson JM. Protein adsorption from human plasma is reduced on phospholipids polymers. J Biomed Mater Res 1991;25:1397–1407.
24. Goda T, Konno T, Takai M, Moro T, Ishihara K. Biomimetic phosphorylcholine polymer grafting from polydimethylsiloxane surface using photo-induced polymerization. Biomaterials 2006;27:5151–5160.
25. Sibarani J, Takai M, Ishihara K. Surface modification on microfluidic devices with 2-methacryloyloxyethyl phosphorylcholine polymers for reducing unfavorable protein adsorption. Colloids Surf B Biointerfaces 2007;54:88–93.
26. Ueda H, Watanabe J, Konno T, Takai M, Saito A, Ishihara K. Asymmetrically functional surface properties on biocompatible phospholipid polymer membrane for bioartificial kidney. J Biomed Mater Res A 2006;77:19–27.
27. Palmer RR, Lewis AL, Kirkwood LC, Rose SF, Lloyd AW, Vick TA, Stratford PW. Biological evaluation and drug delivery application of cationically modified phospholipid polymers. Biomaterials 2004;25:4785–4796.
28. Snyder TA, Tsukui H, Kihara S, Akimoto T, Litwak KN, Kameneva MV, Yamazaki K, Wagner WR. Preclinical biocompatibility assessment of the EVAHEART ventricular assist device: Coating comparison and platelet activation. J Biomed Mater Res A 2007;81:85–92.
29. Kuiper KJ, Nordrehaug JE. Early mobilization after protamine reversal of heparin following implantation of phosphorylcholine-coated stents in totally occluded coronary arteries. Am J Cardiol 2000;85:698–702.
30. Galli M, Sommariva L, Prati F, Zerboni S, Politi A, Bonatti R, Mameli S, Butti E, Pagano A, Ferrari G. Acute and mid-term results of phosphorylcholine-coated stents in primary coronary stenting for acute myocardial infarction. Cathet Cardiovasc Intervent 2001;53:182–187.
31. Lewis AL, Hughes PD, Kirkwood LC, Leppard SW, Redman RP, Tolhurst LA, Stratford PW. Synthesis and characterisation of phosphorylcholine-based polymers useful for coating blood filtration devices. Biomaterials 2000;21:1847–1859.
32. Pavoor PV, Gearing BP, Muratoglu O, Cohen RE, Bellare A. Wear reduction of orthopaedic bearing surfaces using polyelectrolyte multilayer nanocoatings. Biomaterials 2006;27:1527–1533.

AQ1

33. Yamamoto M, Kato K, Ikada Y. Ultrastructure of the interface between cultured osteoblasts and surface-modified polymer substrates. J Biomed Mater Res 1997;37:29–36.

34. Wang P, Tan KL, Kang ET. Surface modification of poly(tetrafluoroethylene) films via grafting of poly(ethylene glycol) for reduction in protein adsorption. J Biomater Sci Polym Ed 2000;11:169–186.

35. Iwata R, Suk-In P, Hoven VP, Takahara A, Akiyoshi K, Iwasaki Y. Control of nanobiointerfaces generated from well-defined biomimetic polymer brushes for protein and cell manipulations. Biomacromolecules 2004;5:2308–2314.

36. Kyomoto M, Iwasaki Y, Moro T, Konno T, Miyaji F, Kawaguchi H, Takatori Y, Nakamura K, Ishihara K. High lubricious surface of cobalt-chromium-molybdenum alloy prepared by grafting poly(2-methacryloyloxyethyl phosphorylcholine). Biomaterials 2007;28:3121–3130.

37. Yoshida K, Greener EH. Effects of coupling agents on mechanical properties of metal oxide-polymethacrylate composites. J Dent 1994;22:57–62.

38. Matinlinna JP, Vallittu PK. Bonding of resin composites to etchable ceramic surfaces—An insight review of the chemical aspects on surface conditioning. J Oral Rehabil 2007;34:622–630.

39. Bryant SJ, Nuttelman CR, Anseth KS. Cytocompatibility of UV and visible light photoinitiating systems on cultured NIH/3T3 fibroblasts in vitro. J Biomater Sci Polym Ed 2000; 11:439–457.

40. ASTM. Annual Book of ASTM Standards, vol. 13: Standard specification for cobalt-28 chromium-6 molybdenum alloy casting and casting alloy for surgical implants (UNS R30075). ASTM; 2004. ASTM F75–01.

41. ASTM. Annual Book of ASTM Standards vol. 13: Standard Practice for Surface Preparation and Marking of Metallic Surgical Implants. ASTM; 2004. ASTM F86–04.

42. Seo M, Sato N. Differential composition profiles in depth of thin anodic oxide films on iron-chromium alloy. Surface Sci 1979;86:601–609.

43. Ishihara K, Iwasaki Y, Ebihara S, Shindo Y, Nakabayashi N. Photoinduced graft polymerization of 2-methacryloyloxyethyl phosphorylcholine on polyethylene membrane surface for obtaining blood cell adhesion resistance. Colloids Surf B Biointerfaces 2000;18:325–335.

44. Kyomoto M, Moro T, Konno T, Takadama H, Yamawaki N, Kawaguchi H, Takatori Y, Nakamura K, Ishihara K. Enhanced wear resistance of modified cross-linked polyethylene by grafting with poly(2-methacryloyloxyethyl phosphorylcholine). J Biomed Mater Res A 2007;82:10–17.

45. Kyomoto M, Moro T, Miyaji F, Hashimoto M, Kawaguchi H, Takatori Y, Nakamura K, Ishihara K. Effect of 2-methacryloyloxyethyl phosphorylcholine concentration on photo-induced graft polymerization of polyethylene in reducing the wear of orthopaedic bearing surface. J Biomed Mater Res A 2008;86: 439–447.

46. Northwood E, Fisher J. A multi-directional in vitro investigation into friction, damage and wear of innovative chondroplasty materials against articular cartilage. Clin Biomech 2007; 22:834–842.

47. ISO. Plastics-film and sheeting-measurement of water-contact angle of corona-treated films. International Organization for Standardization 15989. ISO; 2004.

48. ASTM. Annual Book of ASTM Standards, vol. 13: Standard Test Method for Wear Testing of Polymeric Materials Used in Total Joint Prostheses. ASTM; 2004. ASTM F732–00.

49. Li YS, Tran T, Xu Y, Vecchio NE. Spectroscopic studies of trimetoxypropylsilane and bis(trimethoxysilyl)ethane sol-gel coatings on aluminum and copper. Spectrochim Acta A: Mol Biomol Spectrosc 2006;65:779–786.

50. Matsuda T, Kaneko M, Ge S. Quasi-living surface graft polymerization with phosphorylcholine group(s) at the terminal end. Biomaterials 2003;24:4507–4515.

51. Braunecker WA, Matyjaszewski K. Controlled/living radical polymerization: Features, developments, and perspectives. Prog Polym Sci 2007;32:93–146.

52. Zhang Z, Berns AE, Willbold S, Buitenhuis J. Synthesis of poly(ethylene glycol) (PEG)-grafted colloidal silica particles with improved stability in aqueous solvents. J Colloid Interface Sci 2007;310:446–455.

53. Sakamoto H, Doi H, Kobayashi E, Yoneyama T, Suzuki Y, Hanawa T. Structure and strength at the bonding interface of a titanium-segmented polyurethane composite through 3-(trimethoxysilyl) propyl methacrylate for artificial organs. J Biomed Mater Res A 2007;82:52–61.

54. Tsukagoshi T, Kondo Y, Yoshino N. Protein adsorption and stability of poly(ethylene oxide)-modified surfaces having hydrophobic layer between substrate and polymer. Colloids Surf B Biointerfaces 2007;54:82–87.

55. Puleo DA. Biochemical surface modification of Co-Cr-Mo. Biomaterials 1996;17:217–222.

56. Saldívar-García AJ, Lopez HF. Microstructural effects on the wear resistance of wrought and as-cast Co-Cr-Mo-C implant alloys. J Biomed Mater Res A 2005;74:269–274.

57. Sheeja D, Tay BK, Nung LN Tribological characterization of surface modified UHMWPE against DLC-coated Co-Cr-Mo. Surf Coat Technol 2005;190:231–237.

58. Saikko V. Wear and friction properties of prosthetic joint materials evaluated on a reciprocating pin-on-flat apparatus. Wear 1993;166:169–178.

59. Ishikawa Y, Hiratsuka K, Sasada T. Role of water in the lubrication of hydrogel. Wear 2006;261:500–504.

60. Ho SP, Nakabayashi N, Iwasaki Y, Boland T, LaBerge M. Frictional properties of poly(MPC-co-BMA) phospholipid polymer for catheter applications. Biomaterials 2003;24:5121–5129.

61. Naka MH, Morita Y, Ikeuchi K. Influence of proteoglycan contents and of tissue hydration on the frictional characteristics of articular cartilage. Proc Inst Mech Eng [H] 2005;219: 175–182.

62. Bell CJ, Ingham E, Fisher J. Influence of hyaluronic acid on the time-dependent friction response of articular cartilage under different conditions. Proc Inst Mech Eng [H] 2006;220: 23–31.

63. Kobayashi M, Terayama Y, Hosaka N, Kaido M, Suzuki A, Yamada N, Torikai N, Ishihara K, Takahara A. Friction behavior of high-density poly(2-methacryloyloxyethyl phosphorylcholine) brush in aqueous media. Soft Matter 2007;2: 740–746.

64. Yamamoto S, Ejaz M, Tsujii Y, Fukuda T. Surface interaction forces of well-defined, high-density polymer brushes studied by atomic force microscopy. 2. Effect of graft density. Macromolecules 2000;33:5608–5612.

65. Raviv U, Glasson S, Kampf N, Gohy JF, Jérôme R, Klein J. Lubrication by charged polymers. Nature 2003;425:163–165.
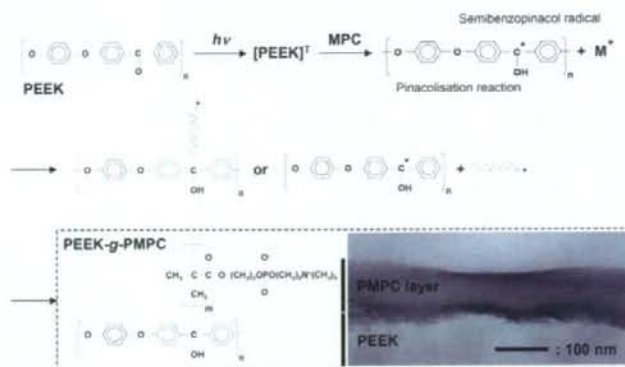
AQ2

Letter

Self-Initiated Surface Graft Polymerization of 2-Methacryloyloxyethyl Phosphorylcholine on Poly(ether ether ketone) by Photoirradiation

Masayuki Kyomoto, and Kazuhiko Ishihara

More About This Article

Additional resources and features associated with this article are available within the HTML version:

- Supporting Information
- Access to high resolution figures
- Links to articles and content related to this article
- Copyright permission to reproduce figures and/or text from this article

View the Full Text HTML

Self-Initiated Surface Graft Polymerization of 2-Methacryloyloxyethyl Phosphorylcholine on Poly(ether ether ketone) by Photoirradiation

Masayuki Kyomoto*,†,‡,§ and Kazuhiko Ishihara†,‖

Research Department, Japan Medical Materials Corporation, 3-3-31 Miyahara, Yodogawa-ku, Osaka 532-0003, Japan, and Department of Materials Engineering, School of Engineering, Division of Science for Joint Reconstruction, School of Medicine, and Center for NanoBio Integration, The University of Tokyo, 7-3-1 Hongo, Bunkyo-ku, Tokyo 113-8656, Japan

ABSTRACT In the present paper, we reported the fabrication of a highly hydrophilic nanometer-scale modified surface on a poly(ether ether ketone) (PEEK) substrate by photoinduced graft polymerization of 2-methacryloyloxyethyl phosphorylcholine (MPC) in the absence of photoinitiators. Photoirradiation results in the generation of semibenzopinacol-containing radicals of benzophenone units in the PEEK molecular structure, which acts as a photoinitiator during graft polymerization. The poly(MPC)-grafted PEEK surface fabricated by a novel and simple polymerization system exhibited unique characteristics such as high wettability and high antiprotein adsorption, which makes it highly suitable for medical applications.

KEYWORDS: poly(ether ether ketone) • phosphorylcholine • surface modification • photopolymerization • wettability • protein adsorption

INTRODUCTION

Poly(aryl ether ketone) (PAEK), including poly(ether ether ketone) (PEEK), is a relatively new family of high-temperature thermoplastic polymers, consisting of an aromatic backbone molecular chain interconnected by ketone and ether functional groups; i.e., a benzophenone (BP) unit is included in its molecular structure. Polyaromatic ketones exhibit enhanced mechanical properties, and their chemical structure is stable at high temperatures, resistant to chemical and radiation damages, and compatible with many reinforcing agents (such as glass and carbon fibers); therefore, they are considered to be promising materials for industrial applications such as aircraft, turbine blades, and electric devices. In the 1990s, the biocompatibility and in vivo stability of various PAEK materials and high-performance engineering polymers were investigated (1). Recently, PEEK has emerged as the leading high-performance thermoplastic candidate for replacing metal implant components, especially in the field of orthopedics and trauma (2). In recent studies, the tribological and bioactive properties of PEEK, which is used as a bearing material and flexible implant in joint arthroplasty, have been investigated (3–5). However, conventional single-component PEEK cannot sat-

isfy these requirements (e.g., wear resistance or fixation with a bone) for the artificial joint (2). Because of interest in further improving implants, the PEEK as biomaterials study has also been focused on the biocompatibility of the polymer, either as a reinforcing agent or as a surface modification (6, 7). Therefore, multicomponent polymer systems have been designed in order to synthesize new multifunctional biomaterials. In order to use PEEK and related composites in novel implant applications, they can be engineered to have a wide range of physical, mechanical, and surface properties.

2-Methacryloyloxyethyl phosphorylcholine (MPC), a methacrylate monomer composed of a phospholipid polar group, which is identical with the neutral phospholipids of cell membranes, is used to synthesize polymer biomaterials having excellent biocompatibility (8–12). MPC polymers, exhibiting a cell membrane like structure, have potential application in various fields such as biology, biomedical science, and surface chemistry because they exhibit several unique properties such as good biocompatibility, high lubricity, low friction, and excellent antiprotein adsorption (8–12).

Surface modification is one of the most important technologies for the preparation of new multifunctional biomaterials. In general, a polymer surface can be modified using the following two methods: (a) surface absorption or reaction with small molecules and (b) grafting of polymeric molecules onto a substrate via a covalent bond. Grafting polymerization is performed most frequently using either of the following methods: (i) surface-initiated graft polymerization termed the "grafting from" method in which the monomers are polymerized from initiators or comonomers and (ii) adsorption of the polymer to the substrate termed the "grafting to"

www.acsami.org
VOL. xxx • NO. xx • 000 • XXXX
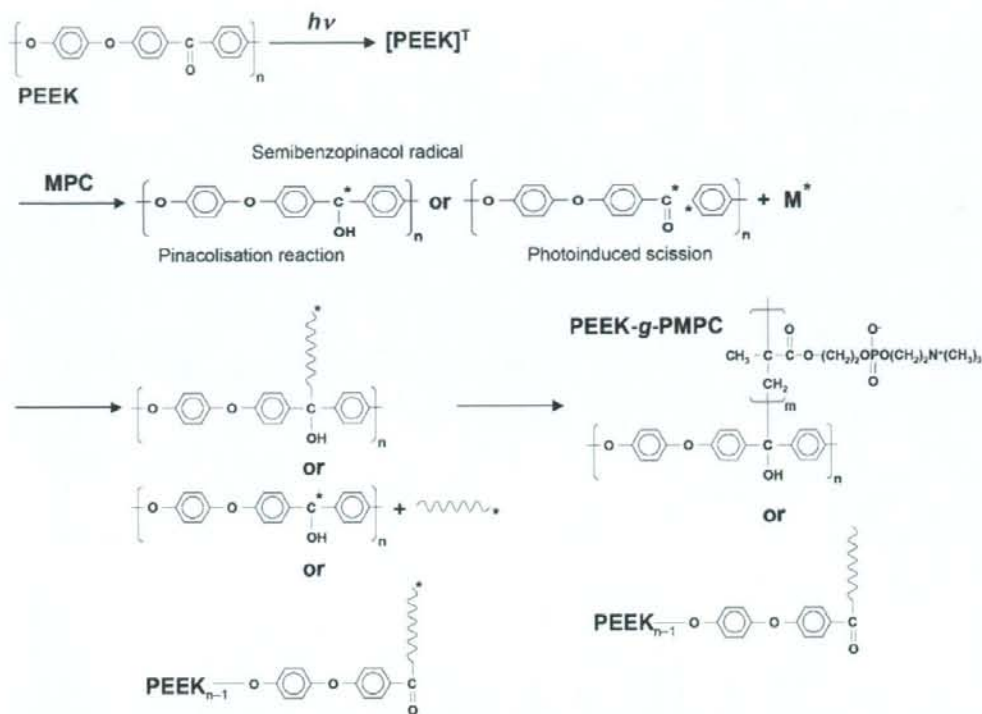APPLIED MATERIALS & INTERFACES   A

FIGURE 1. Scheme for the preparation of PEEK-*g*-PMPC.

methods such as dipping, cross-linking, or reaction of the end groups of the ready-made polymers with the functional groups of the substrate. The "grafting from" method has an advantage over the "grafting to" method in that it forms a high-density polymer brush interface with a multifunctional polymer; this advantage results in a fruitful function. In previous studies, a multifunctional biomaterial such as poly(MPC) (PMPC) was grafted onto a polyethylene (PE) surface; this was accomplished using photoinduced "grafting from" polymerization in the presence of a conventional BP photoinitiator (13−17). During grafting, the physically adsorbed BP initiators on the PE surface were excited to the triplet-state hydrogen (H) atom from the −CH₂− group of the PE surface; this resulted in the formation of radicals that were capable of inducing surface-initiated graft polymerization, which was conducted under ultraviolet (UV) irradiation.

In this study, we have demonstrated the fabrication of a biocompatible and highly hydrophilic nanometer-scale modified surface by grafting PMPC onto the surface of a self-initiated PEEK using a novel photoinduced "grafting from" polymerization reaction. We hypothesize that photoirradiation results in the generation of semibenzopinacol-containing radicals of the BP units in PEEK, which acts as a photoinitiator during the "grafting from" polymerization. It is well-known that when BP is exposed to photoirradiation such as UV irradiation, a pinacolization reaction is induced; this results in the formation of semibenzopinacol (ketyl) radicals that act as photoinitiators. Our technique enables the direct grafting of PMPC onto the PEEK surface in the

absence of a photoinitiator, thereby resulting in the formation of a C−C covalent bond between the PMPC and PEEK substrate. The chemical and physical properties of the PEEK surface were also investigated.

MATERIALS AND METHODS

PMPC Graft Polymerization. The preparation of PMPC-grafted PEEK (PEEK-*g*-PMPC) is schematically illustrated in Figure 1. PEEK specimens were machined from an extruded PEEK (450G; Victrex plc, Thornton-Cleveleys, U.K.) bar stock, which was fabricated without stabilizers and additives. The surfaces of the PEEK specimens were ultrasonically cleaned in ethanol for 20 min and then dried in vacuum. MPC was industrially synthesized using the method reported by Ishihara et al. (8) and supplied by the NOF Corp. (Tokyo, Japan). It was dissolved in degassed water to obtain a 0.5 mol/L aqueous solution; PEEK specimens were immersed in this solution. Photoinduced graft polymerization was carried out at 60 °C for 90 min on the PEEK surface under UV irradiation (UVL-400HA ultrahigh-pressure mercury lamp; Riko-Kagaku Sangyo Co., Ltd., Funabashi, Japan) with an intensity of 5 mW/cm², a filter (model D-35; Toshiba Corp., Tokyo, Japan) was used to restrict the passage of UV light to wavelengths of 350 ± 50 nm. After polymerization, the PEEK-*g*-PMPC specimens were removed from the MPC solution, washed with pure water and ethanol to remove nonreacted monomers and nongrafted polymers, and dried at room temperature. As a reference sample, a PEEK-*g*-PMPC with BP was prepared by PMPC grafting with BP precoating. Before PMPC grafting, the PEEK specimens were immersed in an acetone solution containing 10 mg/mL of BP (Wako Pure Chemical Industries, Ltd., Osaka, Japan) for 30 s and then dried in the dark at room temperature in order to remove the acetone. It was reported that the amount of BP adsorbed on the surface was 3.5×10^{-11} mol/cm² (9).
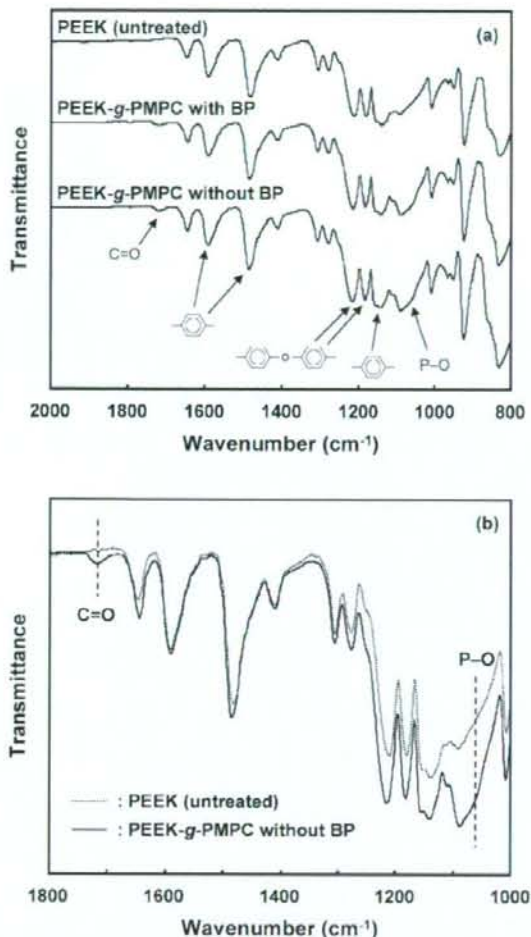
FIGURE 2. FT-IR/ATR spectra of PEEK-*g*-PMPC with/without BP.

Surface Analysis by Fourier Transform Infrared (FT-IR) Spectroscopy, X-ray Photoelectron Spectroscopy (XPS), and Water-Contact Angle Measurement. The functional group vibrations of the PEEK-*g*-PMPC surface that was grafted with/without BP were examined using attenuated total reflection (ATR) by FT-IR spectroscopy. FT-IR/ATR spectra were obtained in 32 scans over a range of 800−2000 cm^{-1} at a resolution of 4.0 cm^{-1} by using an FT-IR analyzer (FT/IR615; Jasco International Co., Ltd., Tokyo, Japan).

The surface elemental contents of the PEEK-*g*-PMPC surface that was grafted with/without BP were analyzed using XPS. XPS spectra were obtained using an XPS spectrophotometer (AXIS Hsi 165; Kratos/Shimadzu Corp., Kyoto, Japan) equipped with a Mg Kα radiation source by applying a voltage of 15 kV at the anode. The takeoff angle of the photoelectrons was maintained at 90°. Each measurement was scanned five times, and five replicate measurements were performed on each sample; their average values were considered for determining the surface elemental contents.

The static water-contact angles of the PEEK-*g*-PMPC surface that was grafted with/without BP were measured with an optical bench-type contact angle goniometer (model DM300; Kyowa Interface Science Co., Ltd., Saitama, Japan) using a sessile drop method. Drops of purified water (1 μL) were deposited on the PEEK-*g*-PMPC surface, and the contact angles were measured directly after 60 s by using a microscope. Subsequently, 15 replicate measurements were performed on each sample, and the average values were taken as the contact angles.

Cross-Sectional Observation of PEEK-*g*-PMPC Using Transmission Electron Microscopy (TEM). The cross section of the PMPC layer fabricated on the PEEK-*g*-PMPC surface that was grafted with/without BP was observed using a transmission electron microscope. First the specimens were embedded in an epoxy resin, stained with a ruthenium oxide vapor at room temperature, and then sliced into ultrathin films (approximately 100 nm thick) using a Leica Ultracut UC microtome (Leica Microsystems, Ltd., Wetzlar, Germany). A JEM-1010 electron microscope (JEOL, Ltd., Tokyo, Japan) was used for TEM observation at an acceleration voltage of 100 kV.

Characterization of Protein Adsorption by a Micro-bicinchoninic Acid (BCA) Method. The amount of protein adsorbed on the untreated PEEK and PMPC layer of the PEEK-*g*-PMPC surface that was grafted with/without BP was measured using the micro-BCA method. Each specimen was immersed in Dulbecco's phosphate-buffered saline (PBS, pH 7.4, ion strength = 0.15 M; Immuno-Biological Laboratories Co., Ltd., Takasaki, Japan) for 1 h to equilibrate the surface modified by the MPC polymer. The specimens were immersed in a bovine serum albumin (BSA; molecular weight = 6.7 × 10^{4}; Sigma-Aldrich Corp., MO) solution at 37 °C for 1 h. The protein solution was prepared in a BSA concentration of 4.5 g/L, i.e., 10% of the concentration of human plasma levels. Then, the specimens were rinsed five times with fresh PBS and immersed in a 1 mass % sodium dodecyl sulfate (SDS) aqueous solution and shaken at room temperature for 1 h to completely detach the adsorbed BSA from the PEEK surface. A protein analysis kit (micro-BCA protein assay kit, no. 23235; Thermo Fisher Scientific Inc., IL) based on the BCA method was used to determine the BSA concentration in the SDS solution, and the amount of BSA adsorbed on the PEEK surface was calculated.

Statistical Analysis. The results derived from each measurement were used to determine the water-contact angle, and the amounts of BSA adsorbed were expressed as mean values and standard deviation. The statistical significance ($p < 0.05$) was estimated by the Student's t test.

RESULTS AND DISCUSSION

In this study, we investigated the PMPC layer formed on the PEEK surface by photoinduced radical graft polymerization in the absence a photoinitiator. The following methods were employed in our study: (a) grafting from polymerization for the formation of a high-density graft polymer layer, (b) photoinduced polymerization in the absence of photoinitiators, and (c) use of biocompatible hydrophilic macromolecules, which exhibited photoreduction by hydrogen abstraction of a BP unit in PEEK from a hydrogen donor; this induced surface-initiated graft polymerization of the methacrylate-type monomer (i.e., MPC) on the PEEK surface, even in the absence of BP as a photoinitiator. These results are discussed hereafter.

The preparation of the PEEK-*g*-PMPC without BP is schematically illustrated in Figure 1. The present graft polymerization reaction involving free radicals is photoinduced by UV irradiation. Under UV irradiation, a BP unit in PEEK can undergo the following reactions in the aqueous MPC solutions (18−24). The pinacolization reaction (photoreduction by hydrogen abstraction of a BP unit in PEEK) results in the formation of a semibenzopinacol radical (i.e., ketyl radical),
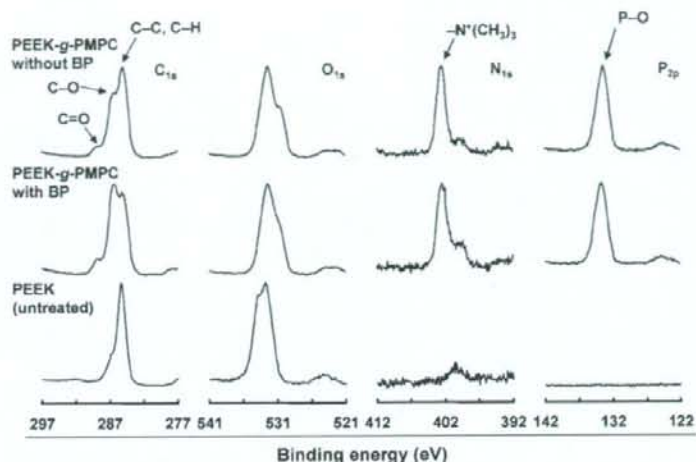
FIGURE 3. XPS spectra of PEEK-*g*-PMPC with/without BP.

Table 1. Surface Elemental Composition ($n = 5$), Static-Water Contact Angle ($n = 15$), and the Amount of BSA Adsorbed ($n = 10$) on PEEK-*g*-PMPC with/without BP

sample	surface elemental composition (atom %)				contact angle (deg)	amount of adsorbed BSA (μg/cm^2)
	C_{1s}	O_{1s}	N_{1s}	P_{2p}		
PEEK (untreated)	83.2 (0.5)^a	16.7 (0.5)	0.1 (0.1)	0.0 (0.0)	92.5 (1.9)	0.42 (0.22)
PEEK-*g*-PMPC with BP	64.5 (1.1)	25.2 (0.8)	5.1 (0.2)	5.2 (0.2)	7.1 (1.1)	0.08 (0.08)
PEEK-*g*-PMPC without BP	62.5 (0.6)	27.3 (0.5)	5.1 (0.1)	5.1 (0.1)	6.8 (1.7)	0.08 (0.10)
PMPC^b	57.9	31.6	5.3	5.3		

^{a} The standard deviation is in parentheses. ^{b} Theoretical elemental composition of PMPC.
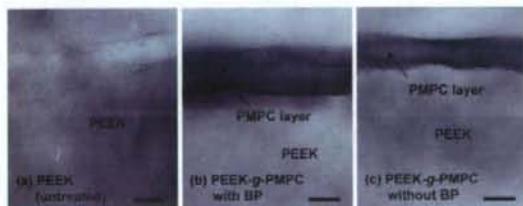

FIGURE 4. Cross-sectional TEM images of PEEK-*g*-PMPC with/without BP. Bar: 100 nm.

which can initiate the "grafting from" polymerization of MPC as the main reaction and the "grafting to" polymerization of MPC (the radical chain end of PMPC couples the semi-benzopinacol radical of the PEEK surface) as a subreaction. In addition, a photoscission reaction occurs as a subreaction, which may not need a hydrogen donor. The cleavage reaction induces recombination and the "grafting from" polymerization. When water polymerization is carried out in the presence of a hydrogen donor, a phenol unit may be subsequentially formed due to hydrogen abstraction.

Figure 2 shows the FT-IR/ATR spectra of untreated PEEK and PEEK-*g*-PMPC with/without BP. Absorption peaks were observed at 1600, 1490, 1280, 1190, and 1160 cm^{-1} for both untreated PEEK and PEEK-*g*-PMPC. These peaks are chiefly attributed to the diphenyl ether group, phenyl rings, or aromatic hydrogen atoms in the PEEK substrate (25, 26). However, transmission absorption peaks at 1720 and 1080

cm^{-1} (shoulder peak) were observed only for PEEK-*g*-PMPC (Figure 2b). These peaks corresponded to the carbonyl group (C=O) and the phosphate group (P–O) in the MPC unit (15–17). The FT-IR/ATR spectra showed no clear difference between PEEK-*g*-PMPC with and without BP.

The XPS spectra of the binding energy region of the nitrogen (N) and phosphorus (P) electrons showed peaks for PEEK and PEEK-*g*-PMPC with/without BP, whereas peaks were not observed in the case of untreated PEEK (Figure 3). The peaks at 403 and 134 eV were attributed to the $-N^+(CH_3)_3$ and phosphate groups, respectively. These peaks indicate the presence of phosphorylcholine in the MPC units. After PMPC grafting, the peaks attributed to the MPC unit were clearly observed in both FT-IR/ATR and XPS spectra of PEEK-*g*-PMPC with/without BP. These peaks indicate that PMPC is successfully grafted on the surface of PEEK (15–17).

Table 1 summarizes the surface elemental compositions of the untreated PEEK and PEEK-*g*-PMPC with/without BP. The elemental compositions of N and P in all of PEEK-*g*-PMPC with/without BP were 5.2 and 5.3 atom %, respectively. The elemental composition of the PEEK-*g*-PMPC surface was almost equal to the theoretical elemental composition (atom %; N, 5.3; P, 5.3) of PMPC. These results indicate that the PMPC layer formed on the PEEK substrate covers fully.

Figure 4 shows the cross-sectional TEM images of the untreated PEEK and PEEK-*g*-PMPC with/without BP. In the

cases of PEEK-*g*-PMPC with/without BP, an approximately 100-nm-thick PMPC layer was clearly observed on the surface of the PEEK substrate, and neither crack nor delamination was observed at the PEEK substrate and the interface between the PMPC layer and the PEEK substrate. These results indicate that the PMPC layer formed on the PEEK substrate is uniformly distributed over the substrate and is bound to the substrate by covalent C−C bonds. Because the photoinduced radical graft polymerization proceeds only on the surface of the PEEK substrate, the properties of the substrate remain unchanged. Retention of the properties of the PEEK substrate is very important in clinical use because the biomaterials used in implants act not only as functional materials but also as structural materials in vivo. During the polymerization of PEEK-*g*-PMPC with BP, the pinacolization reaction was photoinduced (UV irradiation) not only by the BP unit in PEEK but also by the BP initiators precoated on the substrate. However, the amount of semibenzopinacol radicals produced from the BP units in PEEK alone would be sufficient to induce surface-initiated graft polymerization, since there is no clear difference in the PMPC layer between the PEEK-*g*-PMPC with and without BP.

Table 1 summarizes the static water-contact angles and the amount of BSA adsorbed on the untreated PEEK and PEEK-*g*-PMPC with/without BP. The static water-contact angle of the untreated PEEK was 92.5°, and it decreased markedly to 7.1° ($p < 0.001$) and 6.8° ($p < 0.001$), respectively, after PMPC grafting was carried out with/without BP. Because MPC is a highly hydrophilic compound, PMPC is water-soluble (8−12). The water wettability of the PEEK-*g*-PMPC surface was considerably greater than that of the untreated PEEK surface because of the presence of a PMPC nanometer-scale layer (Figure 4). The fluid (water) film forming ability of the PEEK-*g*-PMPC surface can be attributed to such a nanometer-scale thin PMPC layer because the outermost PMPC layer determines this ability. The adsorption of the representative plasma protein and BSA on the PEEK-*g*-PMPC surface considerably decreased to 20% ($p < 0.001$) compared to that in the case of the untreated PEEK (0.08 μg/cm^2). It is hypothesized that the mechanism of protein adsorption resistance on the surface modified by the MPC polymer is attributed to the water structure resulting from the interactions between the water molecules and phosphorylcholine groups (27−30). The presence of a large amount of free water around the phosphorylcholine group is responsible for the easy detachment of proteins and the prevention of conformational changes in the adsorbed proteins (29). A decrease in protein adsorption is also considered to be caused by the presence of a hydrated layer around the phosphorylcholine groups (27). These observations are consistent with the results of the static water-contact angle measurements and cross-sectional TEM observations of the PEEK whose surface is modified by PMPC grafting. These results imply that the PEEK-*g*-PMPC surface is biocompatible in terms of tissue and blood compatibility because MPC polymer modified surfaces are known to exhibit in vivo biocompatibility (8−14).

The novel and simple photoinduced graft polymerization in the absence of photoinitiators would be highly suitable for industrial applications (31, 32) as well as the development of medical devices (2−7). The density and thickness of the grafting layer can be controlled by the photoirradiation time and monomer concentration (16, 17). Additional efforts are needed in this aspect. However, the synthesis of a self-initiated biocompatible polymer having unique properties such as antiprotein adsorption and wettability by the photoinduced "grafting-from" polymerization reaction is indeed a novel and simple phenomenon developed in the field of biomaterials science, and the fabrication of the PEEK-*g*-PMPC surface can result in the development of next-generation multifunctional biomaterials.

CONCLUSION

A biocompatible and highly hydrophilic nanometer-scale modified surface was successfully fabricated on the PEEK substrate by the photoinduced graft polymerization of PMPC in the absence of photoinitiators. Because MPC is a highly hydrophilic compound, the water wettability of the PEEK-*g*-PMPC surface was greater than that of the untreated PEEK surface because of the formation of a PMPC nanometer-scale layer. In addition, the amount of BSA adsorbed on the PEEK-*g*-PMPC surface considerably decreased compared to that in the case of untreated PEEK. This novel and simple photoinduced graft polymerization in the absence of photoinitiators is highly suitable in industrial applications, including the development of medical devices.

REFERENCES AND NOTES

(1) Brown, S. A.; Hastings, R. S.; Mason, J. J.; Moet, A. *Biomaterials* **1990**, *11*, 541−547.
(2) Kurtz, S. M.; Devine, J. N. *Biomaterials* **2007**, *28*, 4845−4869.
(3) Wang, A.; Lin, R.; Stark, C.; Dumbleton, J. H. *Wear* **1999**, 225−229, and 724−727.
(4) Joyce, T. J.; Rieker, C.; Unsworth, A. *Biomed. Mater. Eng.* **2006**, *16*, 1−10.
(5) Latif, A. M. H.; Mehats, A.; Elcocks, M.; Rushton, N.; Field, R. E.; Jones, E. *J. Mater. Sci. Mater. Med.* **2008**, *19*, 1729−1736.
(6) Yu, S.; Hariram, K. P.; Kumar, R.; Cheang, P.; Aik Khor, K. *Biomaterials* **2005**, *26*, 2343−2352.
(7) Fan, J. P.; Tsui, C. P.; Tang, C. Y.; Chow, C. L. *Biomaterials* **2004**, *25*, 5363−5373.
(8) Ishihara, K.; Ueda, T.; Nakabayashi, N. *Polym. J.* **1990**, *22*, 355−360.
(9) Ishihara, K.; Iwasaki, Y.; Ebihara, S.; Shindo, Y.; Nakabayashi, N. *Colloids Surf. B* **2000**, *18*, 325−335.
(10) Kyomoto, M.; Iwasaki, Y.; Moro, T.; Konno, T.; Miyaji, F.; Kawaguchi, H.; Takatori, Y.; Nakamura, K.; Ishihara, K. *Biomaterials* **2007**, *28*, 3121−3130.
(11) Ueda, H.; Watanabe, J.; Konno, T.; Takai, M.; Saito, A.; Ishihara, K. *J. Biomed. Mater. Res. A* **2006**, *77*, 19−27.
(12) Snyder, T. A.; Tsukui, H.; Kihara, S.; Akimoto, T.; Litwak, K. N.; Kameneva, M. V.; Yamazaki, K.; Wagner, W. R. *J. Biomed. Mater. Res. A* **2007**, *81*, 85−92.
(13) Moro, T.; Takatori, Y.; Ishihara, K.; Konno, T.; Takigawa, Y.; Matsushita, T.; Chung, U. I.; Nakamura, K.; Kawaguchi, H. *Nat. Mater.* **2004**, *3*, 829−837.
(14) Moro, T.; Takatori, Y.; Ishihara, K.; Nakamura, K.; Kawaguchi, H. *Clin. Orthop. Relat. Res.* **2006**, *453*, 58−63.
(15) Kyomoto, M.; Moro, T.; Konno, T.; Takadama, H.; Kawaguchi, H.; Takatori, Y.; Nakamura, K.; Yamawaki, N.; Ishihara, K. *J. Mater. Sci. Mater. Med.* **2007**, *18*, 1809−1815.
(16) Kyomoto, M.; Moro, T.; Konno, T.; Takadama, H.; Yamawaki, N.; Kawaguchi, H.; Takatori, Y.; Nakamura, K.; Ishihara, K. *J. Biomed. Mater. Res. A* **2007**, *82*, 10−17.

LETTER

(17) Kyomoto, M.; Moro, T.; Miyaji, F.; Hashimoto, M.; Kawaguchi, H.; Takatori, Y.; Nakamura, K.; Ishihara, K. *J. Biomed. Mater. Res. A* **2008**, *86*, 439–447.

(18) Giancaterina, S.; Rossi, A.; Rivaton, A.; Gardette, J. L. *Polym. Degrad. Stab.* **2000**, *68*, 133–144.

(19) Wang, H.; Brown, H. R.; Li, Z. *Polymer* **2007**, *48*, 939–948.

(20) Yang, W.; Rånby, B. *Eur. Polym. J.* **1999**, *35*, 1557–1568.

(21) Qiu, C.; Nguyen, Q. T.; Ping, Z. *J. Membr. Sci.* **2007**, *295*, 88–94.

(22) Nguyen, H. X.; Ishida, H. *Polymer* **1986**, *27*, 1400–1405.

(23) Cole, K. C.; Casella, I. G. *Thermochim. Acta* **1992**, *211*, 209–228.

(24) Qiu, K. Y.; Si, K. *Macromol. Chem. Phys.* **1996**, *197*, 2403–2413.

(25) He, D.; Susanto, H.; Ulbricht, M. *Prog. Polym. Sci.* **2009**, *34*, 62–98.

(26) Deng, J.; Wang, L.; Liu, L.; Yang, W. *Prog. Polym. Sci.* **2009**, *34*, 156–193.

(27) Goda, T.; Konno, T.; Takai, M.; Ishihara, K. *Colloids Surf. B* **2007**, *54*, 67–73.

(28) Futamura, K.; Matsuno, R.; Konno, T.; Takai, M.; Ishihara, K. *Langmuir* **2008**, *24*, 10340–10344.

(29) Ishihara, K.; Nomura, H.; Mihara, T.; Kurita, K.; Iwasaki, Y.; Nakabayashi, N. *J. Biomed. Mater. Res.* **1998**, *39*, 323–330.

(30) Hoshi, T.; Sawaguchi, T.; Konno, T.; Takai, M.; Ishihara, K. *Polymer* **2007**, *48*, 1573–1580.

(31) Hasegawa, S.; Suzuki, Y.; Maekawa, Y. *Radiat. Phys. Chem.* **2008**, *77*, 617–621.

(32) Chen, J.; Asano, M.; Maekawa, Y.; Yoshida, M. *J. Membr. Sci.* **2008**, *319*, 1–4.